Astronomische Gesellschaft: Reviews in Modern Astronomy

Highlight talk at the annual meeting of the Astronomische Gesellschaft
"The Circuit of Matter", September 2002, Berlin, Germany

Circuit of Dust in Substellar Objects

Christiane Helling

Zentrum für Astronomie und Astrophysik, TU Berlin
Hardenbergstraße 36, 10623 Berlin, Germany

Konrad-Zuse-Zentrum für Informationstechnik Berlin
Takustr. 7, 14195 Berlin, Germany

chris@astro.physik.tu-berlin.de
http://astro.physik.tu-berlin.de/∼chris/

December 5, 2002

Abstract

Substellar atmospheres are cool and dense enough that dust forms very efficiently. As soon as these particles are formed, they sizedependently precipitate due to the large gravity of the objects. Arriving in hot atmospheric layers, the dust evaporates and enriches the gas by those elements from which it has formed. The upper atmospheric layers are depleted by the same elements. Non-continuous and spatially inhomogeneous convective element replenishment, generating a turbulent fluid field, completes the circuit of dust.

The formation of dust in substellar atmosphere is described by extending the classical theory of Gail & Sedlmayr for the case of different gas and dust velocities. Turbulence is modeled in different scale regimes which reveals turbulence as trigger for dust formation in hot environments. Both mechanisms cause the dust to be present in else wise dust-hostile region: precipitation transports the dust into hot regions, and turbulence allows the formation of dust in there.

1 Introduction

The classical problem of stellar atmospheres had been considered as almost solved: observed spectra are reproduced by solving hydrostatic equilibrium equation coupled with a frequency-dependent radiative transfer involving an extensive body of opacity data and a gas phase equilibrium chemistry. Typical examples are A-type stars (e.g. Allard et al. 1998, Castelli & Kurucz 2001) or the carbon-rich AGB stars (e.g. Loidl et al. 2001). Due to the appropriately high precision of such reproductions, synthetic spectra fits can be fully automated as it has been demonstrated in (Bailer-Jones 2000).

This situation changed when the first brown dwarf Gliese 226B was discovered in 1994 and the first spectra became available. At that time, none of the classical model atmosphere simulations were able to reproduce satisfactorily such a substellar atmosphere spectrum. Tsuji et al. (1996) were the first who communicated that important physical effects are very likely correlated with the presence of dust which had not been taken into account in the modeling of substellar objects.

Substellar objects, i.e., brown dwarfs and planets, are high gravity objects with considerable compact atmospheres. Their atmospheres are cool enough that complex molecules are present and phase transitions (*dust formation*) can take place. The carbon is no longer locked into the CO molecules because of the high density of the atmosphere, therefore, molecules like CH_4, CO_2, H_2O, ... appear simultaneously thereby challenging opacity calculations. As soon as solid (or fluid) particles (*dust*) have formed, they will sizedependently precipitate due to the large gravity of the objects. The dust grains will then arrive in an atmospheric layer which is hot enough to evaporate them thermally. The lower atmospheric regions will be enriched by those elements from which the dust grains have formed and the upper atmospheric layers will be depleted by the same. The *circuit of dust in a substellar atmosphere* (Fig. 1) is completed by convective element replenishment. Brown dwarfs are nearly fully convective (see e.g. Chabrier & Baraffe 1997 but Tsuji 2002) which creates a turbulent environment in their atmospheres. Therefore, a non-continuous and spatially inhomogeneous replenishment of the upper atmosphere from deeper layers with those elements previously preticipated can be expected. The dust formation process in hot layers is nevertheless triggered by mixing events due to convective motion. Since the vertical extension of a brown dwarf atmosphere is quite small – typical density scale heights are as small as $H_\rho \approx 10^6\,$cm – all these processes occur in a thin layer, similar to the "weather" in the Earth's atmosphere.

As a consequence, the classical theory of stellar atmospheres misses two major points: i) dust formation with its strong feedbacks on the atmosphere, and ii) dust formation in turbulent gases. Both will be discussed in the following.

2 Key processes of dust formation

According to the classical theory of Gail & Sedlmayr (1984, 1986, 1999), dust formation is to be considered as a two step process: 1) small seed particles (*clusters*) form out of the gas phase (*nucleation*) and 2) subsequently grow to macroscopic sizes (*growth*). A third process influences the dust complex in the gravitationally dominated atmosphere of a substellar object: gravitational settling (*drift*)[1].

[1]Drift occurs if some force on a particle counter balances friction and causes the grains to move with a different velocity than the gas. Examples are the radiation force in red giants or the gravity in substellar objects.

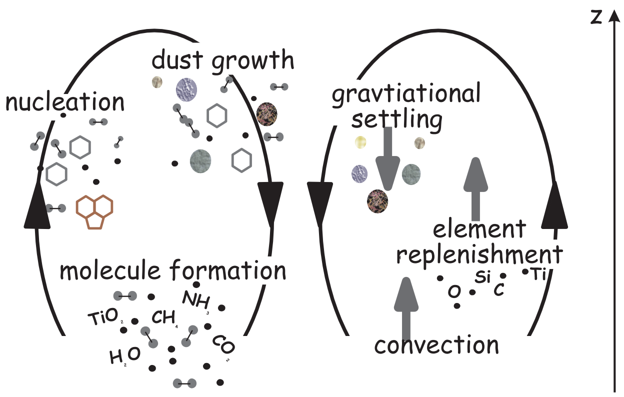

Figure 1: The circuit of dust in substellar atmospheres: dust formation (nucleation, growth) → gravitational settling (drift) → element replenishment by convection → dust formation.

Nucleation: The formation of *seed particles* can in the most simple case be described as a linear reaction chain where the same monomer (e.g. TiO_2, Jeong 2000) is added during each reaction step:

$$A_1 \rightleftharpoons A_2 \rightleftharpoons \cdots \rightleftharpoons A_{N-1} \underset{\tau_{\rm ev}^{N}}{\overset{\tau_{\rm gr}^{N-1}}{\rightleftharpoons}} A_N \underset{\tau_{\rm ev}^{N+1}}{\overset{\tau_{\rm gr}^{N}}{\rightleftharpoons}} A_{N+1} \rightleftharpoons \cdots \rightleftharpoons A_{N_*} \rightleftharpoons \cdots .$$

The first stable cluster (N_*, *critical cluster*) forms if the growth rate $\tau_{\rm gr}$ exceeds the evaporation rate $\tau_{\rm ev}$. Now, the growth of subsequently larger clusters can be considered as a stationary flux through the cluster space from which a *stationary nucleation rate* J_* results.

Growth: Once seed particles are formed, they subsequently grow via chemical reactions on the seed's surface but can only sustain in the gas phase if they are thermally stable. Thermal stability can be visualized by the stability sequence[2] in Fig. 2 where those $(T, n_{<H>})$ are plotted for which the supersaturation ratio $S = 1$. The compounds are stable below $S = 1$ and evaporate at temperatures/densities above such a curve.

Seed particles, which provide the necessary surface for the formation of macroscopic dust grains, are located in the stable growth regime (see Fig. 2) of any stability sequence because a considerable supersaturation is necessary that non-planar particles form from the gas phase. Therefore, many compounds are already thermally stable and rather *heterogeneous core-mantle grains* will form in the atmosphere of a brown dwarf and maybe also in planetary atmospheres.

[2] Stability sequences are not to be confused with condensation sequences.

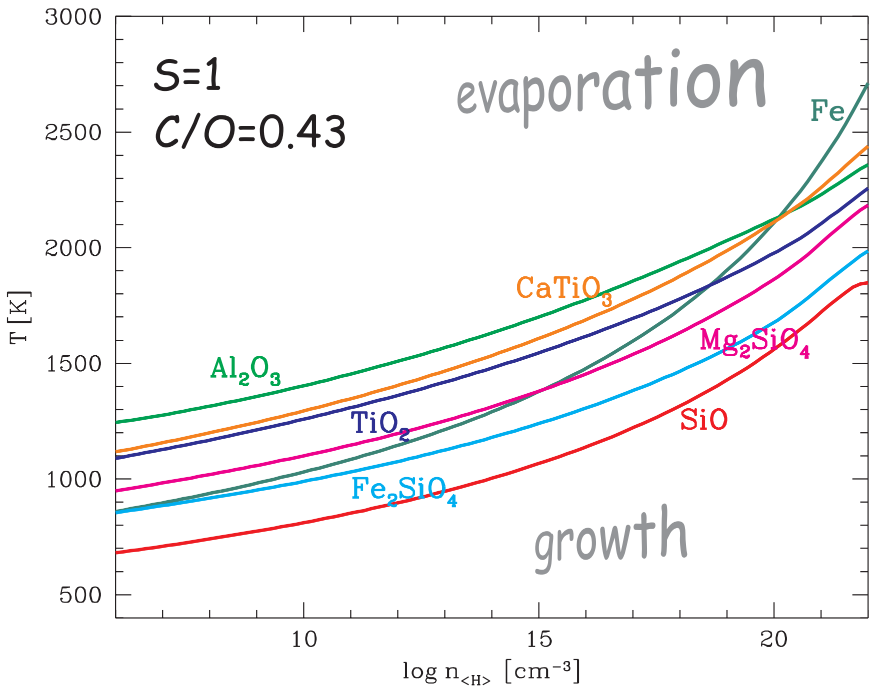

Figure 2: Stability sequence for an oxygen-rich gas (C/O=0.43), typical for a brown dwarf atmosphere.

Gravitational settling: The dust formation process is influenced by drift, i.e., dust and gas move with the different velocities ($\boldsymbol{v}_{\rm dust} = \boldsymbol{v}_{\rm dr} + \boldsymbol{v}_{\rm gas}$) because of the high gravity of substellar objects. It can be shown that the time needed by a particle to reach its final velocity, $\tau_{\rm acc}$, is much smaller than any other time scales involved, i.e. $\min\{\tau_{\rm hyd}, \tau_{\rm gr}, \tau_{\rm sink}\} \gg \tau_{\rm acc}$. Therefore, the *equilibrium drift* concept can be applied where the equilibrium drift velocity, $\boldsymbol{v}_{\rm dr} = \mathring{\boldsymbol{v}}_{\rm dr}$, is implicitly given by the force equilibrium,

$$m_{\rm d}\,\boldsymbol{g}(\boldsymbol{x}) + \boldsymbol{F}_{\rm fric}(\boldsymbol{x}, a, \mathring{\boldsymbol{v}}_{\rm dr}) = 0, \tag{1}$$

where the force of gravity is balanced by the force of friction $\boldsymbol{F}_{\rm fric}(\boldsymbol{x}, a, \mathring{\boldsymbol{v}}_{\rm dr})$. Depending on the hydrodynamic situation, characterized by the Knudsen number $Kn = \bar{l}/(2a)$ ($\bar{l}$ - mean free path, a particle size), different cases need to be considered for the force of friction and also for the dust volume accretion rate dV/dt (compare Eqs. 4, 6):

free molecular flow $Kn \gg 1$		**viscous case** $Kn \ll 1$
subsonic	**force of friction**	laminar
supersonic		turbulent
freely impinging	**volume accretion rate**	diffusive

The volume accretion rate, which defines the particle's growth time scale $\tau_{\rm gr} = \frac{4\pi\, a^3/3}{dV/dt}$, is either determined by molecules freely impinging on the grains surface or by diffusion towards the surface. Aiming at a theoretical description of the dust formation, a typical time which a particle of size a needs to cross a density scale hight H_ρ with a velocity $\mathring{\boldsymbol{v}}_{\rm dr}$, $\tau_{\rm sink} = \frac{H_\rho}{\mathring{\boldsymbol{v}}_{\rm dr}}$, is compared with $\tau_{\rm gr}$ in Fig. 3. Herein, the (a, ρ) plane in Fig. 3 (ρ - gas density) is subdivided by a dashed line where $\tau_{\rm sink} = \tau_{\rm gr}$: Above this line, i.e., where $a > a_{\tau_{\rm sink}=\tau_{\rm gr}}$, the grains would be removed by gravitational settling before they can form, hence, such particle sizes can not exist. Applying a gas density range typically for a brown dwarf atmosphere, the *maximum grain size* $a_{\rm max}$ to be expected depends on the gas density and is 1μm in the cold and thin outer layers and 100μm in the hot and dense layers inside the atmosphere. Furthermore, $\tau_{\rm sink} = \tau_{\rm gr}$ limits the number of hydrodynamical regimes to be expected in a brown dwarf atmosphere: *the subsonic free molecular flow and the laminar viscous flow* need to be considered.

2.1 Theory of dust formation for substellar atmospheres

A theoretical description of the formation of dust in compact, substellar atmosphere, i.e., in gravitationally dominated gases, can be derived by utilizing the key idea of Gail & Sedlmayr (1988) of defining dust moments, $\rho L_j(\boldsymbol{x}, t)$ [cm^j/cm^3],

$$\rho L_j(\boldsymbol{x}, t) = \int_{\infty}^{V_l} V^{j/3} f(V, \boldsymbol{x}, t) dV, \qquad (2)$$

of the grain size distribution function $f(V, \boldsymbol{x}, t)$ and the grain volume V. Allowing – in contrast to Gail & Sedlmayr – for $v_{\rm dust} \neq v_{\rm gas}$, systems of dust moment equations result for the two hydrodynamic cases relevant for a compact atmosphere (Woitke & Helling 2002):

• **subsonic free molecular flow** (Kn$\gg$1 $\wedge$ $\mathring{\boldsymbol{v}}_{\rm dr} \ll c_T$):

$$\frac{\partial}{\partial t}(\rho L_j) + \nabla(\boldsymbol{v}_{\rm gas}\, \rho L_j) \;=\; [{\rm Da}_{\rm d}^{\rm nuc} \cdot {\rm Se_j}]\; J(V_l) + \left[{\rm Da}^{\rm gr}_{\rm d,lKn}\right] \frac{j}{3}\, \chi^{\rm net}_{\rm lKn}\, \rho L_{j-1}$$
$$+ \left[\left(\frac{\pi\gamma}{32}\right)^{1/2} \frac{{\rm M}\cdot{\rm Dr}}{{\rm Kn}^{\rm HD}\cdot{\rm Fr}}\right] \xi_{\rm lKn} \nabla\!\left(\frac{L_{j+1}}{c_T}\,\vec{e}_r\right) \qquad (3)$$

$$\chi^{\rm net}_{\rm sKn} = \sqrt[3]{48\pi^2} \sum_r \Delta V\, n_r\, D_r \left(1 - \frac{1}{S_r}\right) \qquad \xi_{\rm sKn} = \frac{2}{9}\left(\frac{3}{4\pi}\right)^{2/3} g\, \rho_d \qquad (4)$$

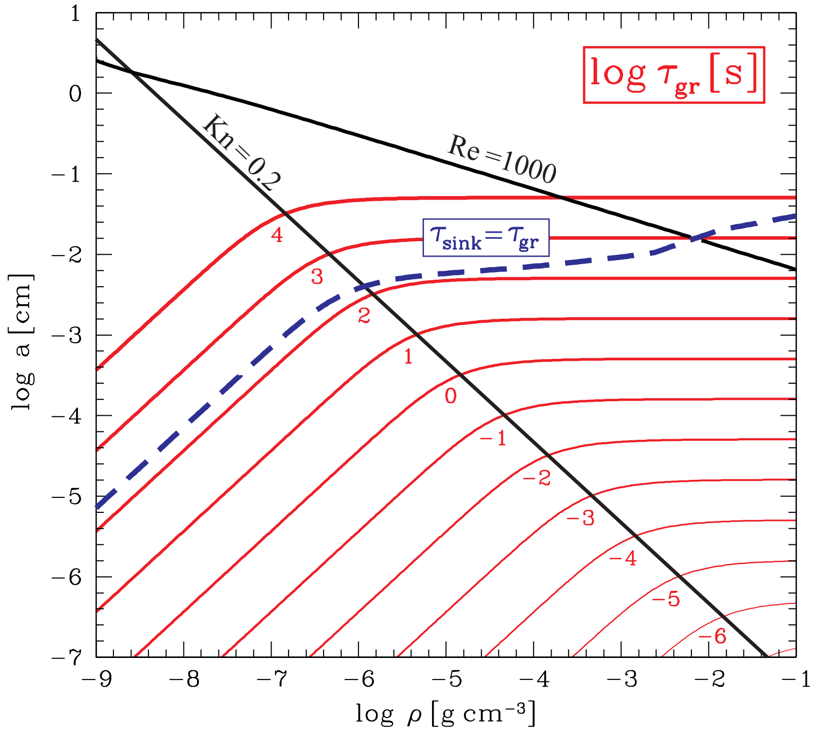

Figure 3: Contour plot of the growth time scale $\log \tau_{\rm gr}$ [s] as function of the grain size a and the gas density ρ at constant temperature $T = 1500\,$K for quartz (SiO_2, $\rho_{\rm d} = 2.65\,{\rm g\,cm^{-3}}$). We assume growth by accretion of the key species SiO with maximum particle density $n_{\rm SiO} = 10^{(7.55-12)} n_{\langle {\rm H}\rangle}$ and extreme supersaturation ($S \to \infty$; for more details see Woitke & Helling 2002).

• **laminar viscous flow**($\mathrm{Kn} \ll 1 \wedge \mathrm{Re_d} < 1000$):

$$\frac{\partial}{\partial t}(\rho L_j) + \nabla(\boldsymbol{v}_{\rm gas}\,\rho L_j) \;=\; [\mathrm{Da_d^{nuc}} \cdot \mathrm{Se_j}]\; J(V_l) + \left[\mathrm{Da^{gr}_{d,sKn}}\right] \frac{j}{3}\, \chi^{\rm net}_{\rm sKn}\, \rho L_{j-2} + \left[\left(\frac{\pi\gamma}{288}\right)^{1/2} \frac{\mathrm{M \cdot Dr}}{\mathrm{Kn \cdot Kn^{HD} \cdot Fr}}\right] \xi_{\rm sKn} \nabla\left(\frac{\rho L_{\rm j+2}}{\mu_{\rm kin}}\, \vec{e}_r\right) \tag{5}$$

$$\chi^{\rm net}_{\rm lKn} = \sqrt[3]{36\pi} \sum_r \Delta V\, n_r v_r^{\rm rel} \alpha_r \left(1 - \frac{1}{S_r}\right) \qquad \xi_{\rm lKn} = \frac{\sqrt{\pi}}{2}\left(\frac{3}{4\pi}\right)^{1/3} g\,\rho_d\;, \tag{6}$$

with $j = 0, 1, 2, \ldots$. The equations reveal the same conservative form with source terms as those in the classical Gail & Sedlmayr case: the first source term on the r.h.s. of Eqs. (3) and (5) represents the nucleation since it contains the nucleation rate J_*. The second source term describes the heterogeneous dust growth with $\chi^{\rm net}$ being the growth speed which depends on the hydrodynamical regime considered (l.h.s. of Eqs. (4) and (6)). By allowing for $v_{\rm dust} \neq v_{\rm gas}$, a third – advective – source term appears which transports already existing particles in regions with possibly still supersaturated gas where they can continue to grow. ξ is the gravitational force density for each of the regimes (r.h.s. of Eqs. (4) and (6)).

The equations (3) and (5) are written *dimensionless*, therefore, characteristic numbers appear in front of the source terms being put in brackets $[\cdot]$ for lucidity[3]. Evaluating the characteristic numbers for a typical brown dwarf model atmosphere, a *hierarchical appearance of the source terms* become evident. If the thermodynamic conditions are appropriate for nucleation, the nucleation source term will determine the solution of the equations. The growth source term becomes most dominant if nucleation becomes inefficient. The advective drift source term determines the solution of the equations only if dust nucleation and growth are negligibly small.

One may, however, observe that the systems of equations (3) and (5) are not closed. Here, further work is necessary but, nevertheless, the closure is possible in the case of a static, stationary subsonic free molecular flow to be demonstrated in the next section. For the general case, one might take notice of the work of Deuflhard & Wulkow (1989) and Wulkow (1992) who adopted orthogonal polynomials of a discrete variable to construct closure terms.

2.2 Formation & structure of a quasi-static cloud layer

The formation and the structure of a quasi-static cloud layer can be investigated by solving the extended dust moment equations (Eqs. 3 - 5). As example, the static ($\boldsymbol{v}_{\rm gas} = 0$), stationary ($\partial/\partial t = 0$) case of Eqs. (3,4) for a subsonic ($\mathring{\boldsymbol{v}}_{\rm dr} \ll c_T$) free molecular flow ($Kn \gg 1$) is presented. The equations have been supplemented with element consumption and a homogeneous gas mixing, and are solved on top of a prescribed brown dwarf atmosphere structure kindly provided by Tsuji (2002). For simplicity, the formation of pure TiO_2-grains is considered where first $(TiO_2)_N$ seed particles form and second, continue to grow a TiO_2 mantle. The homogeneous mixing occurs with a time scale of $\tau_{\rm mix} = 10^4$s in the example presented in Fig. 4.

Five major zones can be distinguished. In *Zone I*, nucleation takes place efficiently due to a very large supersaturation of the gas. Most of the Ti is now locked in the dust which immediately precipitates into deeper layers. Therefore, a depth-dependent depletion of those molecules consumed by dust formation results. In our case, a large depletion of TiO and TiO_2 occurs in the upper zones. In *Zone II*, nucleation is considerably less efficient and this region is determined by the growth of already existing particles. The mean particles size $\langle a \rangle$ increases steeply, and therewith also the mean drift velocity $\langle \mathring{\boldsymbol{v}}_{\rm dr} \rangle$[4]. In the Zones III – V, no dust formation is possible since $J_* = 0$

[3] A detailed description of these characteristic numbers and all other quantities is given in Helling et al. (2002) and Woitke & Helling (2002).

[4] The mean drift velocity, which is calculated according to Eq. (66) in

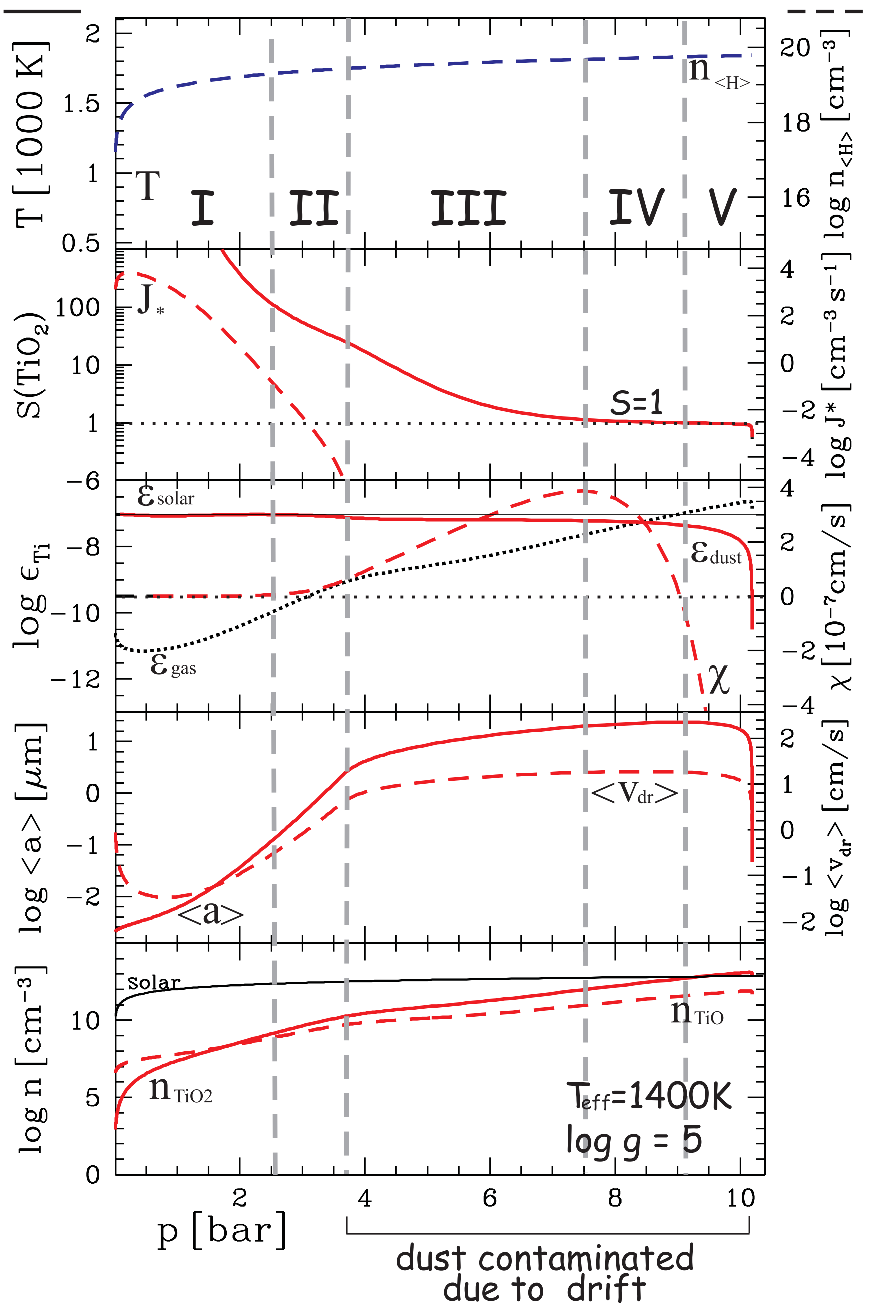

Figure 4: The dust-stratified structure of a quasi-static cloud layer ($T_{\rm eff}$ = 1400K, $\log g$ = 5, $\tau_{\rm mix} = 10^4$s): *Zone I* - nucleation dominated, *Zone II* - growth dominated, *Zone III* - drift dominated, *Zone IV* - saturated rain, *Zone V* - evaporation dominated.

because of the temperature being too high. Therefore, the dust contained in these regions must have formed in the upper layers (Zone I & II). Therefore, *Zone III* is dominated by the drift process which transports dust in regions which are still supersaturated and, therefore, the dust can continue to grow. However, $\langle a\rangle$ increases only slightly and $\langle \mathring{\boldsymbol{v}}_{\rm dr}\rangle$ reaches a terminal value due to the competition between the increasing grain size and the increasing gas density which hinders the dust to move faster inwards. In *Zone IV*, no effective growth takes place since $S \approx 1$. The rain is saturated in these layers. In *Zone V*, temperatures are high enough to evaporate the grains. Consequently, $\langle a\rangle$ and $\langle \mathring{\boldsymbol{v}}_{\rm dr}\rangle$ decrease. Note, that in Zone IV the element abundance in the gas phase, $\varepsilon_{\rm gas}$, exceeds the number of elements locked in the dust grains $\varepsilon_{\rm dust}$, and even the initial solar abundance of the gas phase. This shows that precipitating dust grains have elementally enriched the deepest atmospheric layers causing the molecular abundance to be larger than without precipitating dust.

The consistent description of dust formation, drift and element depletion has provided inside into the formation and the structure of a quasi-static cloud layer which exhibits

- a dust stratified large scale structure where only in the outer regions dust formation is possible. The inner regions are dust contaminated due to drift.
- a depth dependent gas depletion in the upper atmosphere and an enrichment of the deeper atmosphere by heavy elements.

3 Dust formation in turbulent gases

The large scale structure of a dust forming substellar, brown dwarf atmosphere has been investigated by supplying a consistent theoretical description of dust formation in gravitationally dominated media. On such large scales, the atmosphere of a brown dwarf is largely convective. Convection provides a disturbance which is large enough to cause the atmospheric fluid to be highly turbulent because the inertia of the fluid is large compared to its friction ($\Rightarrow$ large Reynolds number).

Turbulence is a multi-scale phenomenon as it was already observed and painted by Leonardo da Vinci (Fig. 5) 500 years ago and as for example observations of Jupiter's surface reveal it today. However, only the largest scales of a turbulent fluid are accessible by any kind of observation (compare Fig. 6). Therefore, observations of brown dwarf variability, e.g., by Bailer-Jones & Mundt (2001), Eislöffel & Scholz (2001), and those of planetary atmospheres reveal merely the large scale structures of the fluid.

Numerical experiments of moderately large Reynolds number flows have shown that the simulation of the largest scales requires only 2% of the whole

Woitke & Helling (2002) adopting the mean particles size $\langle a\rangle$, $\langle \mathring{\boldsymbol{v}}_{\rm dr}\rangle = \frac{\sqrt{\pi} g \rho_{\rm d}}{2\rho c}\langle a\rangle$ ($\rho_{\rm d}$ - grain material density, c - speed of sound).

Figure 5: Leonardo da Vinci (c. 1513, *Old Man with Water Studies*).

computing time. The remaining 98% are necessary to resolve the small scale structures down to the viscous subrange where the energy is dissipated by frictional forces (Dubois, Janberteau & Temam 1999). Therefore, for hydrodynamic simulations one naturally desires to model these scales. In addition, chemical and structure formation processes, like e.g. combustion or dust formation, are seeded in the small scale regime. While the smallest scales may be not considerably influenced by the large scale flow structure (though they are energized by them), the structure formation on the small scales may seed large scale structure formation. Only the latter will be observable but the previous are, nevertheless, needed to reach a detailed understanding of the largest scales and thereby of any observation.

Therefore, the different scale regimes have to be studied in order to reveal the basic physical mechanisms involved in the dust formation in turbulent media.

3.1 Dust formation in the microscopic scale regime

The study of the microscopic regime ($l_{\mathrm{ref}} \ll H_\rho$) provides an unique possibility to gain insight in governing processes involved in structure formation and in particular in the formation of dust in a turbulent fluid since direct numerical simulations of hydrodynamic processes can be carried out. The turbulent

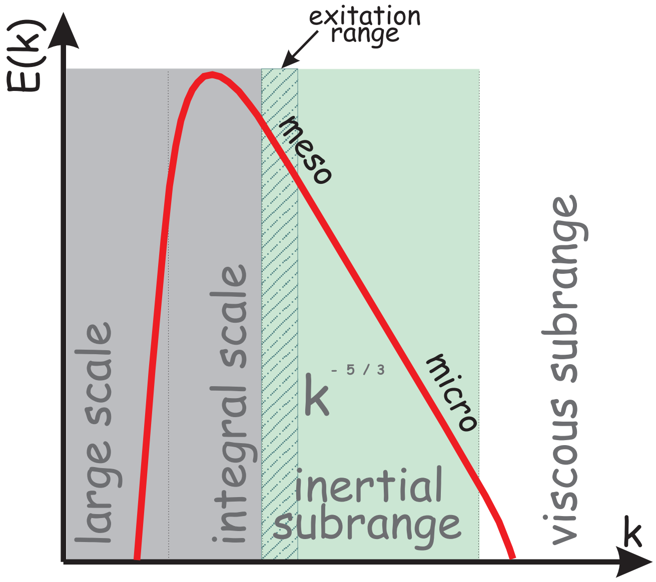

Figure 6: Scale regimes involved in a turbulent fluid field. Driven turbulent is exited in a small wavenumber interval where $k_{\rm min} = 2\pi/(3h)$ and $k_{\rm max} = 2\pi/l_{\rm ref}$ (h - spatial grid resolution).

fluid field is considered to consist of interacting acoustic waves carrying temperature fluctuations as characteristic of the small wavenumber end of the inertial subrange (compare Fig. 6)[5]. Thereby, the superposition of expansion waves causes the local temperature to drop below the nucleation threshold for a short time interval. During this time, seed particles form, persist in the gas phase and continue to grow to macroscopic sizes (Helling et al. 2001). The principal mechanisms can nicely be studied in a 0D model of a gas box after such a superposition since a long term study of the dust complex is possible.

A fully time-dependent solution of the hydrodynamic equations, the energy equation with radiative cooling, the classical Gail & Sedlmayr dust moment equations consistently coupled to the element conservation equation has been obtained by applying a multi-dimensional Euler-solver for compressible fluids (Smiljanovski et al. 1997) and the operator splitting method for the source terms. The coupled complex of classical dust formation, the element consumption and the radiative cooling is solved by the LIMEX DAE solver (Deuflhard & Nowak 1987) for each hydrodynamic time step because of the strong coupling between these equations. LIMEX solves reliably the steady state of the dust complex after the transition from a dynamic (Fig. 7:

[5] Note that the characteristic velocity of a regime is inverse proportional to its characteristic length. Therefore, $v_{\rm ref,micro} = c_s$ in the microscopic regime does not contradict the findings of the mixing length theory since it concerns a macroscopic scale.

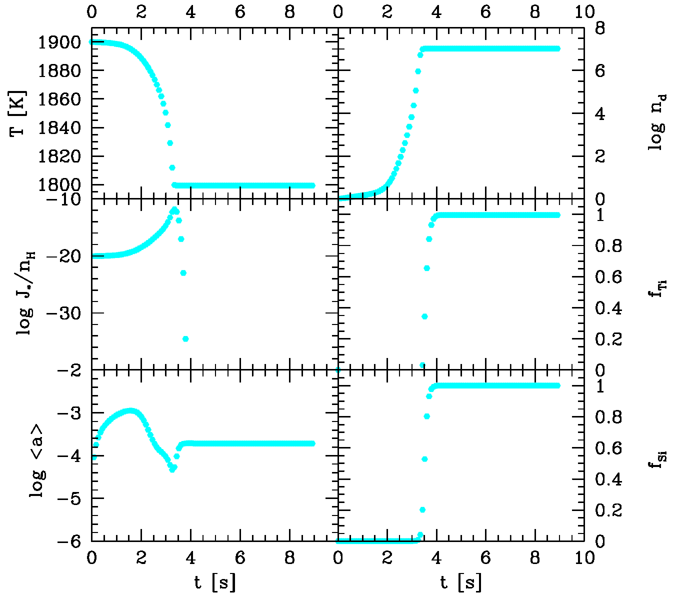

Figure 7: Time evolution of a gas box after an expansion wave superposition staring from the following initial values: $T(x,0) = 1900\,\mathrm{K}$, $\rho(x,0) = 10^{-4}\mathrm{g\,cm^{-3}}$, $\rho(x,0)\,L_0(x,0) = 1\mathrm{cm^{-3}}$, $v_{\rm ref,micro} = 10^4\mathrm{cm\,s^{-1}}$, $l_{\rm ref,micro} = 10^4\mathrm{cm}$; see also Helling et al. (2001) Fig. 3.
(**1st row:** T [K] - gas temperature (l.h.s.), $n_{\rm d}$ [cm^{-3}] - dust particle density (r.h.s); **2nd row:** $J_*/n_{<H>}$ [s^{-1}] - nucleation rate (l.h.s.), $f_{\rm Ti}$ - degree of condensation of Ti (r.h.s.); **3rd row:** $\langle a\rangle$ [10^{-4} cm] - mean grain radius (l.h.s.), $f_{\rm Si}$ - degree of condensation of Si (l.h.s.))

$t < 3.2\,\mathrm{s}$) to an equilibrium situation (Fig. 7: $t > 3.2\,\mathrm{s}$). The simulation now concerns the formation of core-mantel grains made of a TiO_2-seed on which SiO and TiO_2 grow a heterogeneous mantle.

micro-Results: The simulation starts from a temperature much too high for nucleation. But, the small amount of grains formed during a wave superposition event will grow ($\Rightarrow$ increase of $\langle a\rangle$; Fig. 7: 3rd row, l.h.s.). Soon, the particles are large enough that radiative cooling sets in, therefore, the temperature starts to decrease. The larger the initial particles grow, the faster the temperature drops. Finally, the temperature is low enough that nucleation is re-initiated ($\Rightarrow$ increase of J_*; 2nd row, l.h.s.) and the number of dust particles $n_{\rm d}$ increases (1st row, r.h.s.). Now, a *feedback loop* establishes (compare Fig. 10) since more dust intensifies the radiative cooling which causes the temperature to increase even further. Conditions for most efficient nucleation are met, therefore, even more particles form. The process stops if all material

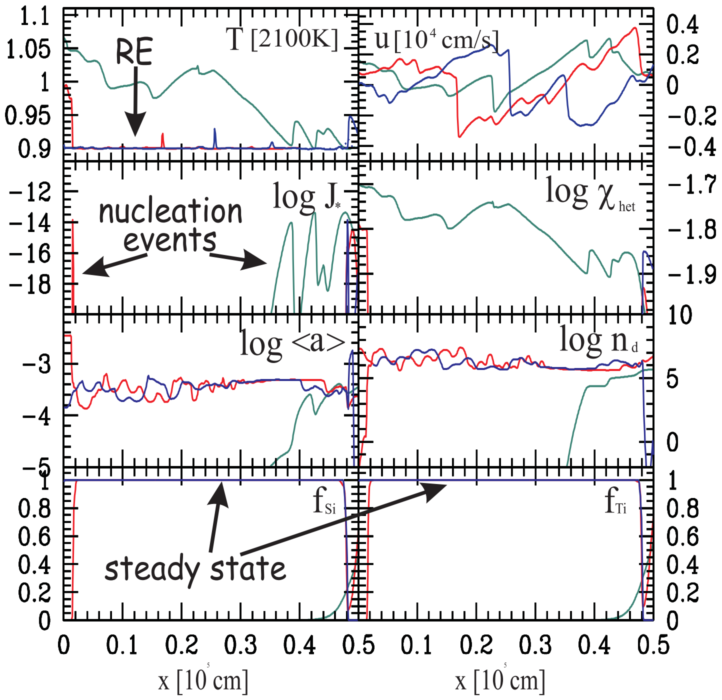

Figure 8: The evolution of the dust complex in space under the conditions of driven turbulence for three time steps. ($T(\boldsymbol{x},0) = 2100\,\mathrm{K}$, $\rho(\boldsymbol{x},0) = 10^{-4}\mathrm{g\,cm^{-3}}$, $v(\boldsymbol{x},0)_{\mathrm{ref,meso}} = 10^{3}\mathrm{cm\,s^{-1}}$, $l_{\mathrm{ref,meso}} = 10^{5}\mathrm{cm}$, $50-k$ mode driven)
(**1st row:** T [K] - gas temperature (l.h.s.), u [10^4 $\mathrm{cm\,s^{-1}}$] - hydrodynamic velocity (r.h.s); **2nd row:** $J_*/n_{<H>}$ [$\mathrm{s^{-1}}$] - nucleation rate (l.h.s.), χ_{het} [cm/s] heterogeneous growth velocity (r.h.s); **3rd row:** $\langle a\rangle$ [10^{-4} cm] - mean grain radius (l.h.s.), n_{d} [1/cm3] - dust particle density (r.h.s); **4th row:** f_{Si} - degree of condensation of Si (l.h.s.), f_{Ti} - degree of condensation of Ti (r.h.s.))

has been consumed, hence, the degree of condensation of the elements involved reaches one ($f_{\mathrm{Ti}}=1$, $f_{\mathrm{Si}}=1$; 2nd and 3rd row, r.h.s.).

3.2 Dust formation in the mesoscopic scale regime

Based on the knowledge gained from the microscale investigations, the scale regime can be extended to larger scales by involving the small wavenumber end of the Kolmogoroff inertial subrange (compare Fig. 6). In this *mesoscopic* regime ($l_{\mathrm{ref}} < H_\rho$) *driven turbulence* is supposed to model a constantly occurring energy input from some convectivly active zone outside a test volume.

In order to fulfill the conservation equations inside the test volume, the stochastic, dust-free velocity, pressure and entropy fields are prescribed on ghost cells located outside the test volume. The stochastic disturbance of the velocity field is, thereby, calculated according to the Kolmogoroff spectrum in the wavenumber space. By solving the hydro-/thermodynamic equations (see Sect. 3.1), the stochastically created waves continuously enter the model volume and, thereby, a turbulent fluid field is generated.

Stochastic boundary conditions driving turbulence: Turbulence is modeled by boundary conditions for our test volume: A disturbance $\delta\alpha(\boldsymbol{x},t)$ is added to a homogeneous background field $\alpha_0(\boldsymbol{x},t)$,

$$\alpha(\boldsymbol{x},t) = \alpha_0(\boldsymbol{x},t) + \delta\alpha(\boldsymbol{x},t). \tag{7}$$

The present pseudo-spectral model for driven turbulence[6] comprises:

• a stochastic distribution of velocity amplitudes $\boldsymbol{\delta v(x,t)}$:

$$\begin{aligned} e(k) &= C_{\mathrm{K}}\varepsilon^{2/3}k^{-5/3} && (8)\\ E^{\mathrm{i}}_{\mathrm{turb}} &= \int_{k_{\mathrm{i+1}}}^{k_{\mathrm{i}}} e(k)\,dk = \frac{3}{2}C_{\mathrm{K}}\varepsilon^{2/3}[k_{\mathrm{i}}^{-2/3} - k_{\mathrm{i+1}}^{-2/3}] && (9)\\ A_{\mathrm{v}}(k_{\mathrm{i}}) &= \sqrt{2z_3E^{\mathrm{i}}_{\mathrm{turb}}} && (10)\\ \delta\boldsymbol{v}(\boldsymbol{x}) &= \Sigma_{\mathrm{i}}\,A_{\mathrm{v}}(k_{\mathrm{i}})\cos(k_{\mathrm{i}}\hat{\boldsymbol{k}}_{\mathrm{i}}\boldsymbol{x} + \omega_{\mathrm{i}}t + \varphi_{\mathrm{i}})\hat{\boldsymbol{k}}_{\mathrm{i}} && (11) \end{aligned}$$

The turbulent energy $E^{\mathrm{i}}_{\mathrm{turb}} = A_{\mathrm{v}}(k_{\mathrm{i}})^2/2$ according to the Kolmogoroff spectrum is assumed to be the most likely value around which a stochastic fluctuation is generated by a Gaussian distributed number z_3 according to the Box-Müller formula $z_3 = \sqrt{-2\log z_1}\sin(\pi z_2)$. z_1 and z_2 are equally distributed random numbers. The random numbers are chosen once at the beginning of the simulation. ε is the energy dissipation rate, $C_{\mathrm{K}} = 1.5$ the Kolmogoroff constant (Dubois, Janberteau & Temam 1999), $k_{\mathrm{i}} = |k_{\mathrm{i}}\hat{\boldsymbol{k}}_{\mathbf{i}}|$ are N equidistantly distributed wavenumbers in Fourier space ($i = 1,\ldots N$ with N the number of modes), and $\varphi_{\mathrm{i}} = 2\pi\, z_4$ are the equally distributed random phase variations. From dimensional arguments the *dispersion relation* $\omega_{\mathrm{i}} = (2\pi\, k_{\mathrm{i}}^2\varepsilon)^{1/3}$ was derived.

• a stochastic distribution of pressure amplitudes $\boldsymbol{\delta P(x,t)}$:

The pressure amplitude is determined depending on the wavenumber of the velocity amplitude $A_{\mathrm{v}}(k_{\mathrm{i}})$ such that the compressible and the incompressible limits are matched for the smallest and the largest wavenumber:

$$A_{\mathrm{P}}(k_{\mathrm{i}}) = \frac{[k_{\mathrm{max}} - k_{\mathrm{i}}]\,\rho A_{\mathrm{v}}(k_{\mathrm{i}})^2 + [k_{\mathrm{i}} - k_{\mathrm{min}}]\,\rho c_{\mathrm{s}} A_{\mathrm{v}}(k_{\mathrm{i}})}{[k_{\mathrm{max}} - k_{\mathrm{min}}]}. \tag{12}$$

[6] For examinations concerning the forcing in direct numerical simulations of turbulence see Eswaran & Pope (1988).

The Fourier cosine transform (as Eq. 9) provides $\delta P(\boldsymbol{x},t)$ in ordinary space. $k_{\rm max} = 2\pi/(3h)$ is the maximum wavenumber with h the spatial grid resolution, $k_{\rm min} = 2\pi/l_{\rm ref}$ is the minimum wavenumber with $l_{\rm ref}$ the size of test volume.

• a stochastic distribution of the entropy $S(\boldsymbol{x},t)$:

The entropy $S(\boldsymbol{x},t)$ is a purely thermodynamic quantity and a distribution can in principle be chosen independently on the distribution of the hydrodynamic quantities. For a given entropy $S(\boldsymbol{x},t)$ and given $P(\boldsymbol{x},t)$ the gas temperature $T(\boldsymbol{x},t)$ is given by:

$$\log T(\boldsymbol{x},t) = \frac{S(\boldsymbol{x},t) + R\log P(\boldsymbol{x},t) - R\log R}{c_{\rm V} + R}\,. \tag{13}$$

So far, $S(\boldsymbol{x},t)$ has been kept constant. R is the ideal gas constant, $c_{\rm V} = 3\,k/(2\mu)$ the specific heat capacity for an ideal gas, k the Boltzmann constant, and $\mu = 2.3\,m_{\rm H}$ the mean molecular weight.

meso-Results: Figure 8 exhibits the principal behavior of the dust complex under the conditions of driven turbulence as function of the horizontal position for three different time steps. The turbulent fluid field creates a strongly fluctuating velocity field and singular temperature decreases which are low enough to cause singular nucleation events. The feedback loop described in Sect. 3.1 causes the temperature to reach its radiative equilibrium quite soon and only small spikes indicate a short deviation due to interacting compression waves. The stochastic appearance of nucleation events results in an rather *inhomogeneous number and mean particle size as function of horizontal position and time* (3rd row). If all condensible material has been consumed, the dust complex has reached a steady state. Further incoming waves will only transport but not modify the dust grains.
In the long term run, the dust complex is characterized by small fluctuation in the mean particles size $\langle a\rangle$ ($\log\langle a\rangle \approx -3.5 \pm 0.25$) and number density $n_{\rm d}$ ($\log n_{\rm d} \approx 6 \pm 1$).

It is, however, possible to gain some inside by calculating mean quantities as for instance in Fig. 9 the space means of all the time steps available for the simulation in Fig. 8. Figure 9 depicts the resulting quantities for the dust complex. One observes large variations in the means of the mean particle radius $\langle\langle a\rangle\rangle$ and the grain number density $\langle n_{\rm d}\rangle$ in the beginning of the calculation but some kind of saturation with only slight variations in the long term run. Only the nucleation rate $\langle J_*\rangle$ and the heterogeneous growth velocity $\langle \chi_{\rm het}\rangle$ fluctuate largely in time which is correlated to the inflow of dust free material from the boundaries into the test volume.

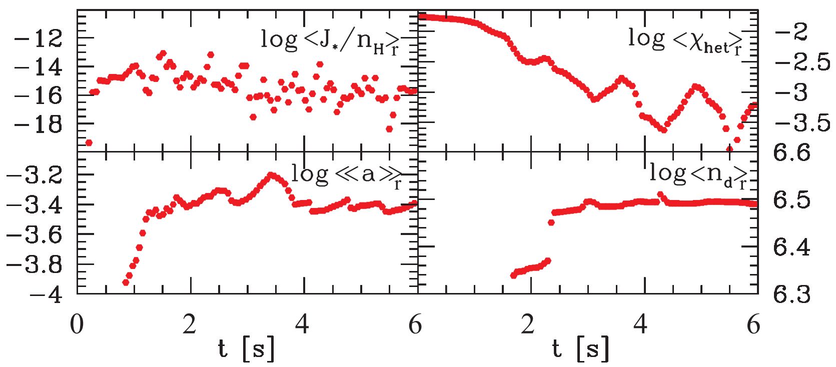

Figure 9: Space mean values of the dust properties as function of time from the simulations depicted in Fig. 8. (**1st row:** $J_*/n_{<H>}$ [1/s] - nucleation rate (l.h.s.), $\chi_{\rm het}$ [cm/s] heterogeneous growth velocity (r.h.s); **2nd row:** $\langle a\rangle$ [10^{-4} cm] - mean grain radius (l.h.s.), $n_{\rm d}$ [1/cm^3] - dust particle density (r.h.s))

4 Summary

The dust formation in substellar objects is presently approximated quite roughly in the context of the classical stellar atmosphere and synthetic spectrum calculations. Often, a fixed particle size or the ISM grain size distribution are assumed. More elaborate treatments apply time scale arguments based on the work of Rossow (1978). Authors assume the presence of homogeneous dust particles made of, e.g., pure iron, and dust condensation is considered independently from gravitational settling.

We have argued, that the **dust in brown dwarf atmospheres**

- consists of **heterogeneous core-mantel grains** because of the necessity of the creation of a first seed particle out of the gas phase. Many compounds are then already stable and grow therefore efficiently on such first surfaces.

- has a **maximum possible mean grain size** between 1μm outside and 100μm inside the atmosphere caused by the equilibrium between gravity and friction.

- **precipitates into dust-hostile region**. Therefore, the site of dust formation does not coincide with the site of maximum dust content in the atmosphere.

- has to be treated consistently with element consumption and precipitation (drift). A **depth-dependent depletion** of molecules results in the upper atmospheric regions while an enrichment results for the innermost atmosphere.

In extension to the classical theory of dust formation developed by Gail & Sedlmayr, the **theory of dust formation in gravitationally dominated gases** allows for different velocities of dust and gas, and thereby

- can rely on the equilibrium drift concept, since the acceleration time scale $\tau_{\rm acc}$ of the dust particles is very small.
- provides a simultaneous description of nucleation, growth, drift, and evaporation by means of systems of moment equations.

Only the largest structures of a turbulent fluid field are observationally accessible but structure formation processes are seeded in the regime of the small, microscopic scales (but $l_{\rm ref} > \eta$, η dissipation length). Dust formation in a turbulent compact atmosphere

- proceeds via a **run away process** which is governed by an unstable **feedback loop** (Fig. 10): The more dust is present, the more efficient the radiative cooling decreases the temperature. More dust forms which again intensifies the radiative cooling (Fig. 10).

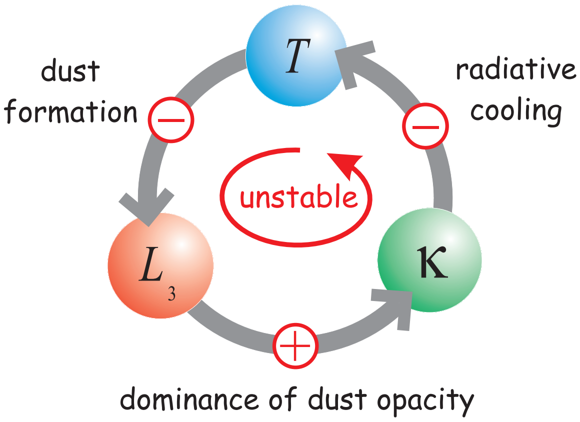

Figure 10: Unstable feedback loop

- occurs via **stochastic nucleation events** due to stochastically superimposed waves.
- results in an **inhomogeneous distribution** of dust in spaces and time, size and number.

5 Conclusion

The circuit of dust in substellar atmospheres is influenced on the macroscopic scales by convective upwelling which provides an efficient mechanism to elementally enrich the upper atmospheric regions. These regions have been depleted by precipitating dust which simultaneously continues to grow on its way into the deeper atmosphere. On the small scales, a turbulent fluid field influences the dust formation process creating random dust formation events. Both mechanisms cause the dust to be present in elsewise dust-hostile regions: precipitation transports the dust into hot regions, and turbulence allows the formation of dust in there.

Acknowledgement: I thank R. Klein for many enlightning and guiding discussions. I thank him and B. Patzer for careful reading the manuscript. This work has been supported by the *DFG* (grands SE 420/19-1, 19-2; Kl 611/7-1, 9-1). Most of the literature search has been performed with the ADS system.

References

Allard N. F., Drira, I., Gerbaldi M., Kielkopf J., Spielfiedel A., 1998, A&A 335, 1124
Bailer-Jones C. A. L., Mundt R., February 2001, A&A 367, 218
Bailer-Jones C. A. L., 2000, A&A 357, 197
Castelli F., Kurucz R., 2001, A&A 372, 260
Chabrier G., Baraffe I., 1997, A&A 327, 1039
Deuflhard P., Wulkow M., 1989, IMPACT Comp. Sci. Eng. 1, 269
Deuflhard P., Nowak U., 1987, In Deuflhard P., Engquist B., *Large Scale Scientific Computing. Progress in Scientific Computing 7*, 37. Birkhäuser
Dubois, T., Janberteau, F., Temam, R., 1999, *Dynamic Multilevel Methods and the Numerical Simulaion of Turbulence*, Cambridge University Press
Eislöffel J., Scholz A., 2001, In Alves J., *The Origins of Stars and Planets: The VLT View*, in press
Gail H.-P., Sedlmayr E., 1986, A&A 166, 225
Gail H.-P., Sedlmayr E., 1988, A&A 206, 153
Gail H.-P., Sedlmayr E., 1999, A&A 347, 594
Gail H.-P., Keller R., Sedlmayr E., 1984, A&A 133, 320
Helling Ch., Oevermann M., Lüttke M., Klein R., Sedlmayr E., 2001, A&A 376, 194
Jeong K. S., 2000, *Dust shells around oxygen–rich Miras and long–period variables*, PhD thesis, Technische Universität, Berlin, Germany
Loidl R., Lanǫn A., Jørgensen U., 2001, A&A 371, 1065
Rossow W. V., 1978, Icarus 36, 1
Smiljanovski V., Moser V., Klein R., 1997, Combustion Theory & Modelling 1, 183
Tsuji T., 2002, ApJ 575, 264
Tsuji T., Ohnaka K., Aoki W., 1996, A&A 305, L1
Woitke P., Helling Ch., 2002, A&A, in press
Wulkow M., 1992, IMPACT Comp. Sci. Eng. 4, 153